

## Chapter 6

### Double condensate experiments – phase related [3]

The relative quantum phase between two Bose-Einstein condensates is expected to give rise to a variety of interesting behaviors, most notably those analogous to the Josephson effects in superconductors and superfluid  $^3\text{He}$  [40]. Experiments with condensates realized in the dilute alkali gases [36, 54, 43] have recently drawn considerable theoretical attention, with a number of papers addressing schemes [88, 83, 123] by which to measure the relative phase. Two independent condensates are expected to possess [41] (or develop upon measurement [87, 49]) a relative phase which is essentially random in each realization of the experiment. The experimental observation at MIT of a spatially uniform interference pattern formed by condensates released from two independent traps confirms the existence of a single relative phase [14]. In the next three chapters the phase is measured and manipulated in ways which have strong analogies to liquid helium physics. In this first experiment, we use an interferometric technique to measure the relative phase (and its subsequent time-evolution) between two trapped condensates [15] that are created with a particular relative phase. This system permits us to characterize the effects of couplings to the environment on the coherence [16] between the condensates.

As in our previous work [105, 76], we create a condensate of approximately  $5 \times 10^5$  Rb-87 atoms, confined in the  $|F = 1, m_f = -1\rangle$  ( $|1\rangle$ ) state in a TOP mag-

netic trap. The rotating magnetic field ( $\nu_{\text{AF}} = 1800$  Hz) is ramped to 3.4 G and the quadrupole gradient to 130 G/cm, resulting in a trap with an axial frequency  $\nu_z = 59$  Hz. The fields are chosen to make the hyperfine transition frequency nearly field-independent [75]. We create the second condensate by applying a short ( $\sim 400$   $\mu\text{s}$ ) two-photon pulse that transfers 50% of the atoms ( $\frac{\pi}{2}$ -pulse) from the  $|1\rangle$  spin state to the  $|F = 2, m_F = 1\rangle$  ( $|2\rangle$ ) spin state. The coupling drive has an effective frequency of 6834.6774 MHz and is detuned slightly ( $\sim 100$  Hz) from the expected transition frequency in our trap [17]. After an evolution time  $T$  and an optional second  $\frac{\pi}{2}$ -pulse, we release the condensates from the trap, allow them to expand, and image either of the two density distributions [105]. The post-expansion images preserve the relative positions and gross spatial features of the condensates as they were in the trap [76, 18].

The evolution of the double condensate system, including the coupling drive, is governed by a pair of coupled Gross-Pitaevskii equations for condensate amplitudes  $\Phi_1$  and  $\Phi_2$ :

$$i\hbar\dot{\Phi}_1 = (T + V_1 + U_1 + U_{12})\Phi_1 + \frac{\hbar\Omega(t)}{2}e^{i\omega_{\text{rf}}t}\Phi_2 \quad (6.1)$$

and

$$i\hbar\dot{\Phi}_2 = (T + V_2 + V_{\text{hf}} + U_2 + U_{21})\Phi_2 + \frac{\hbar\Omega(t)}{2}e^{-i\omega_{\text{rf}}t}\Phi_1 \quad (6.2)$$

where  $T = -(\hbar^2/2m)\nabla^2$  is the kinetic energy,  $m$  is the mass of the Rb atom,  $V_{\text{hf}}$  is the magnetic field-dependent hyperfine splitting between the two states in the absence of interactions, condensate mean-field potentials are  $U_i = 4\pi\hbar^2 a_i n_i/m$  and  $U_{ij} = 4\pi\hbar^2 a_{ij} n_j/m$ ,  $n_i = |\Phi_i|^2$  is the condensate density, and the intraspecies and interspecies scattering lengths [105, 76] are  $a_i$  and  $a_{ij} = a_{ji}$ . For the trap parameters given above, the harmonic magnetic trapping potentials  $V_1$  and  $V_2$  are displaced from one another by 0.4  $\mu\text{m}$  along the axis of the trap [75]. The coupling drive is represented here in the rotating wave approximation and is characterized

by the sum of the microwave and rf frequencies,  $\omega_{\text{rf}}$ , and by an effective Rabi frequency  $\Omega(t)$ , where

$$\Omega(t) = \begin{cases} 2\pi \cdot 625 \text{ Hz}, & \text{coupling drive on;} \\ 0, & \text{coupling drive off.} \end{cases} \quad (6.3)$$

Phase-sensitive population transfer between the  $|1\rangle$  and  $|2\rangle$  states occurs with the drive on, but the two condensates become completely distinguishable once the drive is switched off [76]. The first  $\frac{\pi}{2}$ -pulse [Fig. 6.1(b)] creates the  $|2\rangle$  condensate with a repeatable and well-defined relative phase with respect to the  $|1\rangle$  condensate at  $t = 0$ . The relative phase between the two condensates subsequently evolves at a rate proportional to the local difference in chemical potentials between the two condensates  $\omega_{21}(\vec{r}, t)$ , which in general is a function of both time and space. Couplings to the environment [20] can induce an additional (and uncharacterized) diffusive precession of the relative phase, leading to an rms uncertainty in its value  $\Delta\varphi_{\text{diff}}$  [101, 21]. After an evolution time  $T$ , therefore, the condensates have accumulated a relative phase  $\int_0^T \omega_{21}(\vec{r}, t) dt + \Delta\varphi_{\text{diff}}(T)$ . During the same time, the coupling drive accumulates a phase  $\omega_{\text{rf}}T$ . A second  $\frac{\pi}{2}$ -pulse [Fig. 6.1(e)] then recombines the  $|1\rangle$  and  $|2\rangle$  condensates, comparing the relative phase accumulated by the condensates to the phase accumulated by the coupling drive. The resulting phase-dependent beat note is manifested in a difference in the condensate density between the two states. Immediately after the second pulse the density in the  $|2\rangle$  state ( $n_{2f}$ ) is

$$n_{2f}(\vec{r}) = \frac{1}{2}n_1(\vec{r}) + \frac{1}{2}n_2(\vec{r}) + \sqrt{n_1(\vec{r})n_2(\vec{r})} \cos \left[ \left( \int_0^T \omega_{21}(\vec{r}, t) dt \right) - \omega_{\text{rf}}T + \Delta\varphi_{\text{diff}}(T) \right]. \quad (6.4)$$

In this equation,  $n_i$  denote the densities prior to the application of the second  $\frac{\pi}{2}$ -pulse. The interference term in Eq. 6.4 shows that measurement of  $n_{2f}(\vec{r})$  in the overlap region is sensitive to the relative phase. Each realization of the experiment (with a freshly-prepared condensate) yields a measurement of the relative phase

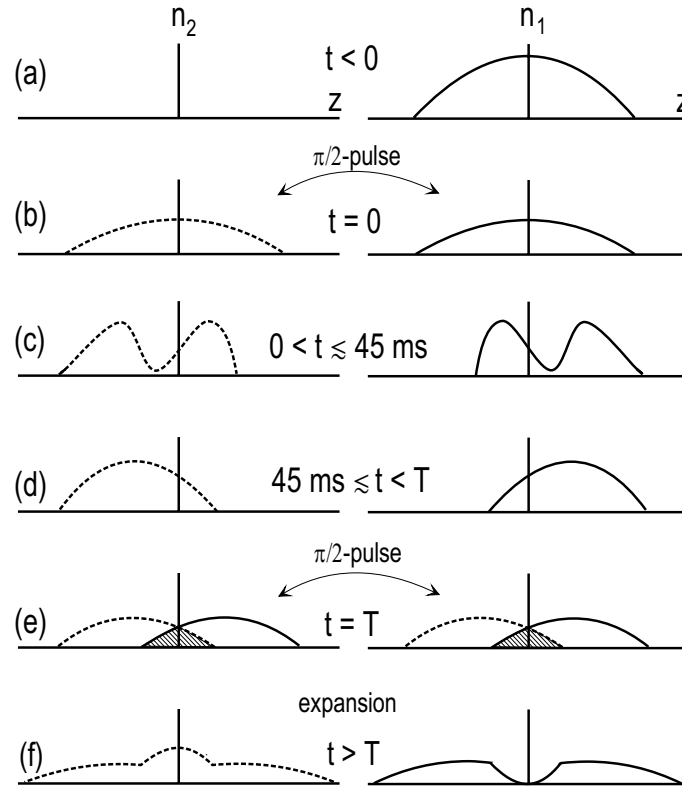


Figure 6.1: A schematic of the condensate interferometer [19]. (a) The experiment begins with all of the atoms in condensate  $|1\rangle$  at steady-state. (b) After the first  $\frac{\pi}{2}$ -pulse, the condensate has been split into two components with a well-defined initial relative phase. (c) The components begin to separate in a complicated fashion due to mutual repulsion as well as a  $0.4 \mu\text{m}$  vertical offset in the confining potentials (see also Fig. 3 of Ref. [76]). (d) The relative motion between the components eventually damps with the clouds mutually offset but with some residual overlap. Relative phase continues to accumulate between the condensates until (e) at time  $T$  a second  $\frac{\pi}{2}$ -pulse remixes the components; the two possible paths by which the condensate can arrive in one of the two states in the hatched regions interfere. (f) The cloud is released immediately after the second pulse and allowed to expand for imaging. In the case shown, the relative phase between the two states at the time of the second pulse was such as to lead to destructive interference in the  $|1\rangle$  state and a corresponding constructive interference in the  $|2\rangle$  state.

for a particular  $T$ ; by varying  $T$ , we can measure the evolution of the relative phase.

At short times  $T$ , for which the overlap between the condensates remains high, varying the moment at which the second  $\frac{\pi}{2}$ -pulse is applied causes an oscillation of the total resulting number of atoms in the  $|2\rangle$  state. The oscillation occurs at the detuning frequency  $\delta = \omega_{21} - \omega_{\text{rf}}$  and is completely analogous to that observed in separated-oscillatory-field measurements in thermal atomic beams [121] or in cold (but noncondensed) atoms in a magnetic trap [50]. The fringe contrast, initially 100%, decreases as the condensates separate. After  $\sim 45$  ms the relative center-of-mass motion damps and comes to equilibrium, leaving the components with a well-defined overlap region at their boundary, as shown in Figs. 6.1(d) and 6.2(a); see also Fig. 5(b) of Ref. [76]. Application of a second  $\frac{\pi}{2}$ -pulse at  $T > 45$  ms results in a density profile in which the interference occurs only in the overlap region; see Figs. 6.1(f) and 6.2(b). We look at the density of atoms in the  $|2\rangle$  state at the center of the overlap region [22] in order to examine the intriguing issue of the reproducibility of the relative phase accumulated by the condensates during the complicated approach to equilibrium. If the phase diffusion term in Eq. 6.4 is so large that the uncertainty is greater than  $\pi$ , then repeated measurements for the same values of  $T$  will yield an incoherent (*i.e.*, random) ensemble of interference patterns. In the opposite extreme, (*i.e.*, very little phase diffusion), repeated measurements will give essentially the same interference pattern at  $T$  in each experimental run. We plot the optical density in the center of the overlap region as a function of  $T$  in Fig. 6.3, and observe an oscillation at the detuning frequency with a visibility of approximately 50%, corresponding to an rms phase diffusion  $\Delta\varphi_{\text{diff}}(T) < \frac{\pi}{3}$ . At longer times the maximum contrast observed in a single realization of the experiment decreases slightly, possibly due to the increasing presence of thermal atoms as the condensates decay.

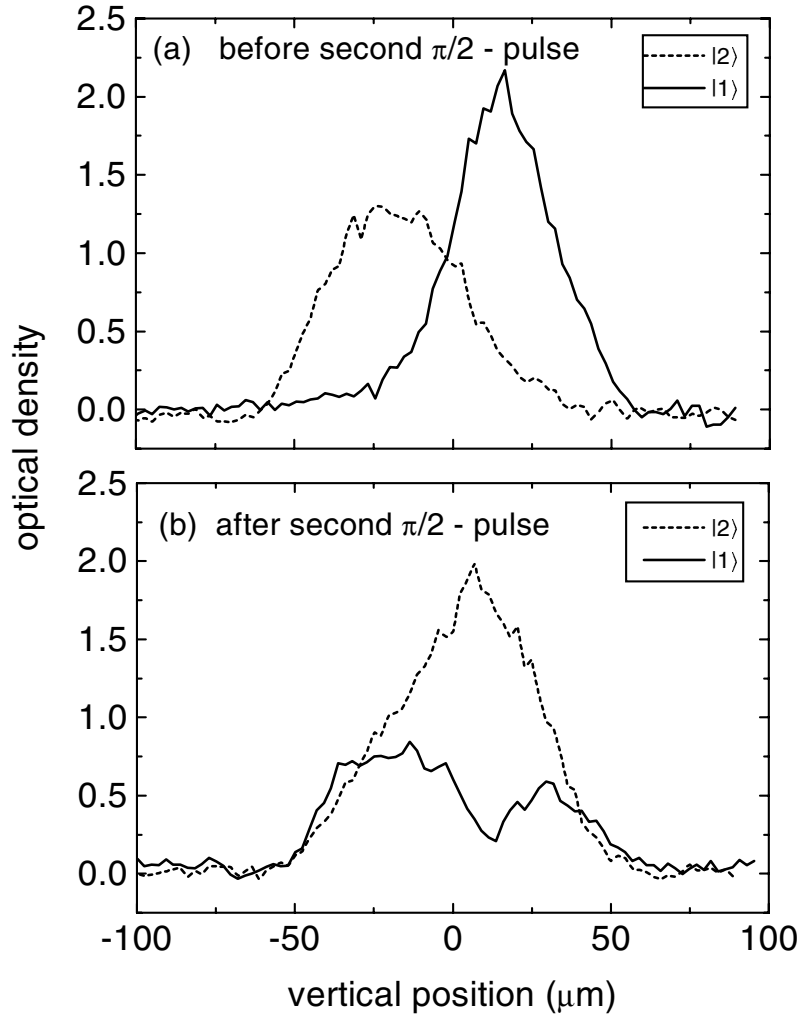


Figure 6.2: (a) The post-expansion density profiles of the condensates in the steady-state attained after a single  $\frac{\pi}{2}$ -pulse. These density profiles vary little from shot-to-shot (and day-to-day). (b) The density profiles after the second  $\frac{\pi}{2}$ -pulse. The density in the overlap region depends on the relative phase between the two condensates at the time of the pulse; in the case shown, we observe constructive interference in the  $|2\rangle$  state and destructive interference in  $|1\rangle$ . The patterns in (b) are much less stable than those in (a), possibly as a result of unresolved higher-order condensate excitations, issues associated with the expansion, or technical instabilities of the apparatus.

The stable interference patterns show that the condensates retain a clear memory of their initial relative phase despite the complicated rearrangement dynamics of the two states following the first  $\frac{\pi}{2}$ -pulse. This is rather surprising, since the center-of-mass motion of the double condensate system is strongly (and completely) damped, and, in general, decoherence times in entangled states tend to be much shorter than damping times [48, 132, 44]. The intuition one develops in understanding few-particle quantum mechanics may not apply to experiments involving condensates. The phase between the two condensates seems to possess a robustness which preserves coherence in the face of the “phase-diffusing” couplings to the environment.

The oscillation pattern of Fig. 6.3 seems to wash out by 100 ms. The peaks and valleys still retain nearly the full contrast, but any given location in time will show a random phase relationship between the two condensates. This can be explained as a  $\pi$  variation in phase at 100 ms, implying a  $2\pi \times 5 \text{ Hz} \times \hbar$  variation in the relative energy of the two condensates. This is likely due to magnetic field fluctuations instead of phase diffusion or decoherence from thermal atoms [71]. For the trap of 130 G/cm and a rotating field of 3.4 G, the field sensitivity of the two-photon transition is  $\sim 250 \text{ Hz/G}$ , implying field fluctuations of 20 mG. A 10% variation in the quadrupole, and a 0.6% variation in the rotating field magnitude can explain this if the time scale is between  $\sim 100 \text{ ms}$  and  $\sim 3 \text{ minutes}$ . If it were faster than 100 ms it would average out, and if it were longer than 3 minutes, we would notice that successive shots were reproducible. Measurements indicate that a 10% variation of the quadrupole field is unreasonable, but the rotating field changes by 1 to 2 % on a time scale of  $\sim 200 \text{ ms}$ . It is therefore very reasonable that our system has irreproducible phase from technical issues.

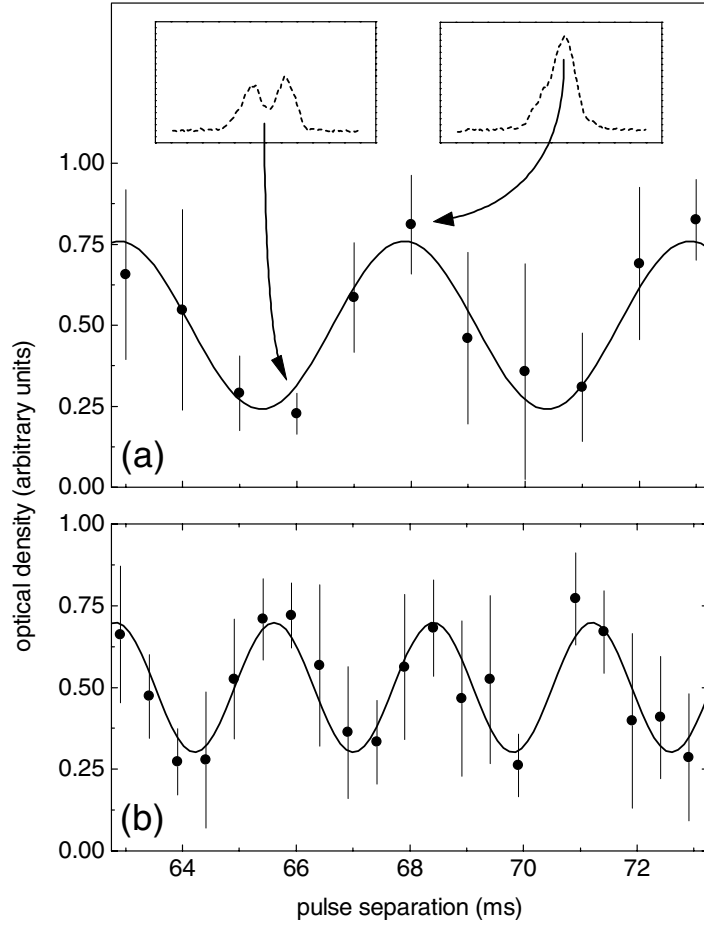


Figure 6.3: The value of the condensate density in the  $|2\rangle$  state is extracted at the center of the overlap region (inset) and plotted (a) as a function of  $T$ . Each point represents the average of 6 separate realizations and the thin bars denote the rms scatter in the measured interference for an individual realization. The thick lines are sinusoidal fits to the data, from which we extract the angular frequency  $\omega_{21} - \omega_{\text{rf}}$ . In (b), the frequency of the coupling drive  $\omega_{\text{rf}}$  has been increased by  $2\pi \cdot 150$  Hz, leading to the expected reduction in fringe spacing.